SimBuild
2024

Eleventh National Conference of IBPSA-USA
Denver, Colorado
May 21 – 23, 2024

An Integrated System for Improving 3D Concrete Printing Process

Chengde Wu[1] and Pete Evans[1]
[1]Iowa State University, Ames, IA

Abstract

3D Concrete Printing (3DCP) is an emerging field that utilizes existing Fused Deposition Modeling (FDM) technologies to automate the building construction process. There are many similarities between conventional FDM technologies and 3DCP technologies, such as hardware design and software workflow, but there are also many differences. Due to the use of concrete as the printing material, the 3D concrete printing workflow cannot adopt the FDM printing workflow without modifications. This research investigated a new integrated system for the 3DCP process to improve the reliability of the 3DCP process. The system includes a slicer module, a path verification module, a g-code generation module, and a scaled physical printing procedure. A pilot study showed that this integrated system can screen certain human-made errors and improve the success rate of 3D concrete printing tasks.

Introduction

3D printing technology was introduced by Hideo Kodama (1981) and then developed into stereolithography by Charles Hull in 1983 (Lengua 2017). 3D Concrete Printing (3DCP) was first proposed in 2001 as Contour Crafting (Luo 2020) to automate the building construction process. In 2014, the first full-scale residential buildings were completed with 3D construction printing (Wu et al. 2016). Currently, there are 130 3D-printed buildings globally (Cobod 2023). Many advances and developments have continued that claim the benefits of 3DCP to include reduced formwork, labor, environmental impacts, and construction time (Wu et al. 2016). Today, the use of the 3DCP technology in the building industry is largely in a nascent state with only limited industry examples and companies achieving a Technology Readiness Level (TRL) of 6-7 on a scale of 1 - 9 and mostly limited to proprietary materials and machines (Ma et al. 2022).

There are multiple categories of 3DCP machines in general, such as Delta, Gantry, Cartesian, and Transforming (telescopic) gantry "Stewart" platforms (ISO/ASTM 2023). The majority utilize cartesian g-code as in the existing Fused Deposition Modeling (FDM) technologies. There are many similarities between conventional FDM technologies and 3DCP technologies, such as hardware design and software workflow, but there are also many differences. One of the primary differences is the printing material. Conventional FDM printers typically use thermoplastics, such as PLA, ABS, etc., while 3D concrete printers use concrete mixes specifically designed for 3D printing. Unlike FDM printing, which has seen significant improvement in the past decades, 3DCP technology is in its infancy and there are many potential failure points. Figure 1 shows an example of a 3D concrete printing job in progress right before it collapsed.

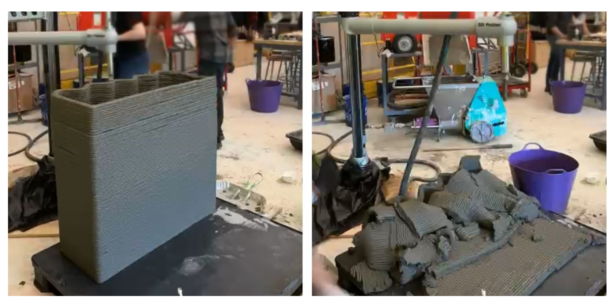

Figure 1 3D Concrete Printing in progress (left) and after collapsed (right).

Due to the use of concrete as the printer material, 3DCP has many challenges, such as energy efficiency (Wu et al. 2023), hygrothermal performance (Ghaderi et al. 2024), carbon footprint (Bukkapatnam et al. 2017). Wu et al. (2023) studied the thermal performance of 3DCP walls using computer simulations with Therm, a thermal transfer model developed by Lawrance Berkeley National Lab. The results indicate that the primary factor that affects the energy performance of 3DCP walls is the thermal bridges from concrete that connect the exterior and the interior concrete layers.

In addition, compared to typical concrete, 3D-printed concrete has to meet stricter requirements to achieve extrudability, buildability, and interlayer bonding strength (Hou et al. 2020). Extrudability refers to the ability of fresh concrete to be transported through a printer nozzle as a continuous filament. It requires concrete to be homogeneous without any blockage, cracking, or segregation. Buildability refers to the ability to bear its weight and the weight of printed layers above without collapsing or excessive deformation during printing. In addition to adequate yield strength and rapid gain in compressive strength to bear the weight, it also requires immediate deformation right after extrusion to be predictable. Interlayer bonding strength is primarily dependent on the interval time between the layers, but the properties of concrete, such as thixotropic properties and surface moisture content, also greatly affect interlayer bonding strength. Thixotropy is a time-dependent shear thinning property. Certain gels or fluids – such as concrete - that are thick or viscous under static conditions will flow over time when shaken, agitated, shear-stressed, or otherwise stressed. They then take a fixed time to return to a more viscous state. 3DCP needs to satisfy the above-mentioned criteria for a controlled and predictable 3DCP construction.

Another factor that leads to failed 3D concrete printing jobs is the current error-prone CAD to CAM workflow. The workflow for FDM printers has been continuously developed in the past decades and established reliable workflow that is standardized and automated. Due to the differences in the material use, 3D concrete printing workflow cannot adopt FDM printing workflow without modifications. The thermoplastic filament used in FDM printers is easily measurable and controllable. The FDM printers can control the filament to feed forward, stop, or retract, and measure the volume of the material being extruded. On the other hand, 3D concrete printers can feed material forward but not backward, and many of them do not have the function to effectively stop the material feed. Mixer, pump, and printer are the three essential components of the 3DCP process, but there is no information exchange between the three components to effectively control material flow. This is because the three components are often engineered by different manufacturers and designed on different platforms. In addition, there are other reasons that the 3DCP process cannot directly adopt the FDM process. For example, FDM printers can utilize support materials to print geometries that are not vertically stacked but support materials cannot be applied to the 3DCP process with the current technology. To overcome these challenges, there is a need to develop a workflow that is better suited for the 3DCP process. The goal of this research is to investigate a new integrated system for the 3DCP process to improve the reliability of the 3DCP tasks.

Literature Review

A common digital process in CAM (Computer-aided Manufacturing) is to convert solid geometries into tool paths based on various parameters such as the size and shape of the tooltips, extrusion or subtraction height, etc. This conversion process is used for CNC routers, robotic arms, and 3D printers. As an additive manufacturing technique, 3D concrete printing also utilizes the same geometry conversion process. Many researchers and industry entities have been researching geometry slicing algorithms and developing software applications to adapt existing technologies to 3DCP constructions.

Xu et al. (2022) investigated a comprehensive 3DCP workflow with a case study in Wujiazhuang, China. In addition to hardware systems, site planning, material design, and structural analysis, this study also explored the software system that utilized vertical extrusions along the X, Y, and Z axes. They 3D printed vault roofs that were fitted onto the walls with mortise-tenon joints. The roofs were printed as vertically extruded arcs on the ground and then lifted and rotated to fit onto the walls. Breseghello and Naboni (2022) studied a toolpath-based fabrication workflow to optimize printing geometry tool paths of structural members and thus optimize the stress of the members and provide design flexibility. They 3D-printed a concrete beam with added tensile members as the pilot study and conducted structural simulation with finite element analysis. Weng et al. (2021) explored a digital workflow that extracts toolpath information from a Building Information Modeling (BIM) tool. BIM is a comprehensive building information management system that is often used by architects and engineers for building design and various simulation purposes. Weng et al., developed a custom software using Dynamo in Revit, a commonly used BIM authoring tool, to extract the geometries from the BIM model, convert them to toolpaths, and test printed a concrete wall at the size of 800mm x 500mm x 1000mm.

There are also commercial software applications for 3DCP workflow and geometry slicing. Chysel is a slicing software application for 3DCP workflow developed by CyBe Construction (CyBe Construction 2024). The cost of a commercial license is €1,500/year. Chysel works on the Rhino/Grasshopper platform and can easily convert geometries into toolpaths by providing the parameters of the 3D concrete printer, such as nozzle size, layer height, etc. Fusion 360, developed by Autodesk (2004), is another software application that incorporated the CAM digital workflow for 3DCP. Fusion 360 is an integrated design-to-manufacturing environment where users can design the geometries of the building components, convert the geometries to toolpaths, and send the information to a 3D concrete printer as g-code, a common file format for 3D printing.

Researchers and industry partners have advanced 3DCP technologies substantially in recent years. One of the missing elements in the existing studies and software applications for 3DCP technologies is the capability to evaluate the challenges of printing slanted walls and thus improve the printing success rate. This can provide architects with more freedom in design and further amplify the advantages of 3DCP technologies. This study investigates a digital and a physical process to improve the success rate of the 3DCP process.

Methodology

This research investigates an integrated system that improves the reliability of the 3DCP process. The system includes a slicer module, a path verification module, and a g-code generation module that generates two g-code files, one for 3DCP and the other for scaled FDM printing. The scaled FDM model is used for physical verification of the printing tool paths. The software used in this research includes Rhino 7, a NURBS-based modeling platform, and Grasshopper, a visual scripting environment in Rhino 7 for parametric modeling.

Slicer Module

The slicer module creates tool paths based on the input geometries, nozzle radius, and layer height. These inputs are provided by the user based on building design and the physical dimensions of the 3D concrete printer. Given a wall geometry in Rhino (figure 2-a), the slicing module first generates a bounding box of the wall (figure 2-b). On the front surface of the bounding box, a series of lines are then generated, with the interval between the lines set to layer height (figure 2-c). The total number of lines is determined by the height of the wall. The lines are scaled to be slightly longer than the length of the bounding box to prevent unexpected results caused by numerical precision issues. The lines are then projected onto the wall geometry horizontally to create initial tool paths (figure 2-d). The tool paths are offset inwards by the radius of the nozzle (figure 2-e). Conventionally when architects design a building, the geometry represents the exterior surfaces of buildings. On the other hand, tool paths represent the center of the 3D printer nozzle. By offsetting the initial paths inwards by the radius of the nozzle, the exterior surface of the 3D-printed wall will match the digital surface in the Rhino model. The final step is to merge all tool paths into one continuous tool path. Figure 2-f shows the nozzle moving along the Z-direction, marked inside the red square.

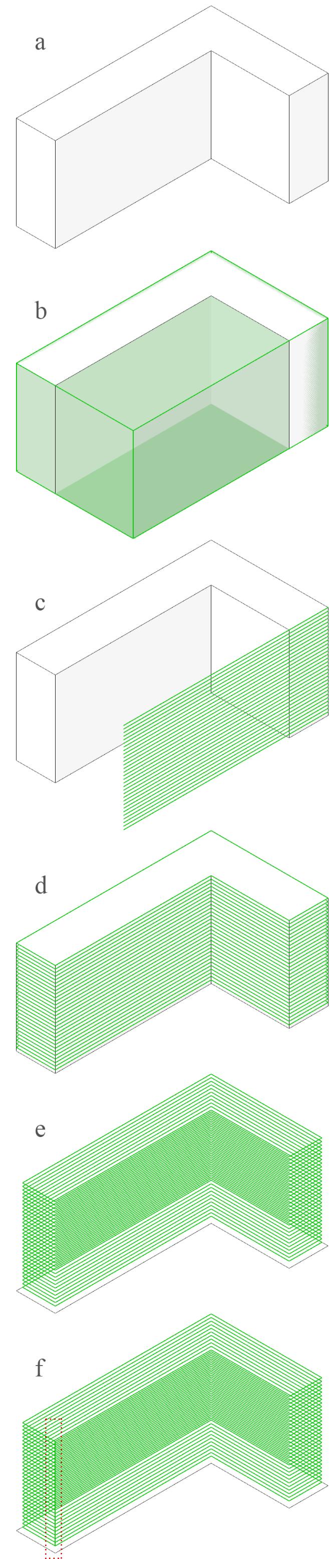

Figure 2 Step-by-step process of the slicer module creating tool paths from a surface geometry

Path Verification Module

One of the benefits of 3DCP is that it provides architects the freedom to design certain curvilinear walls. The primary restriction to the curved walls is the lean angle which is the deviation of the surface of the wall from the vertical axis as shown in figure 3. Due to the absence of formwork and the flowability of the wet concrete, excessive lean angle may cause the collapse of the wall during printing. As a rule of thumb, the 3DCP community typically adopts 15 degrees as the max lean angle.

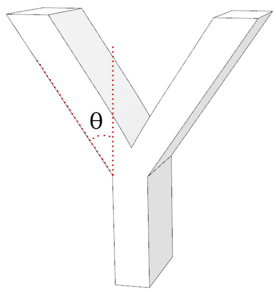

Figure 3 The lean angle Theta denotes the deviation of printing material from the vertical axis

When designing non-vertical walls, it is essential for designers to investigate whether the lean angle of any given point on the wall exceeds the allowed limit. We integrated a lean angle analysis function into the path verification module. The tool paths (red lines in figure 4) created by the slicing module are divided into smaller line segments. The normal vectors (the green arrows in figure 5) of the surface at the endpoints of the line segments are then calculated. If the angle between the normal vectors and the horizontal plane exceeds the maximum allowed lean angle, the printed wall is susceptible to collapsing. This provides designers feedback to adjust the wall designs to meet the physical limitations of the 3DCP technology.

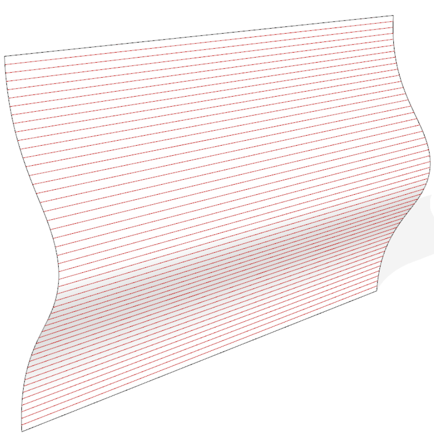

Figure 4 Tool paths on the surface shown in red lines

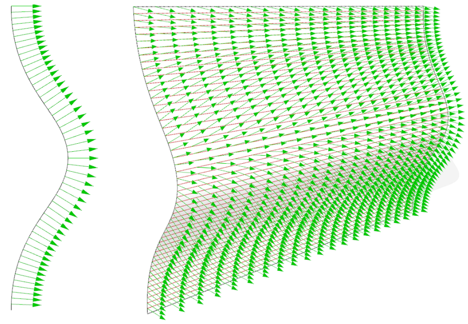

Figure 5 Normal vectors of the surface at the end points of the tool paths shown in section (left) and perspective (right). The normal vectors are used to assess lean angles.

Visually inspecting wall designs is not always accurate or intuitive. For example, between the two walls shown in figure 6 below, Wall A shows reasonable curvature with mild changes in tool paths while Wall B shows much more drastic changes in the printing tool paths. However, the tool path verification module shows that the lean angle of any given point on wall B is under the limit while the lean angle of many points on Wall A exceeds the maximum allowed lean angle, as shown in red dots in figure 7.

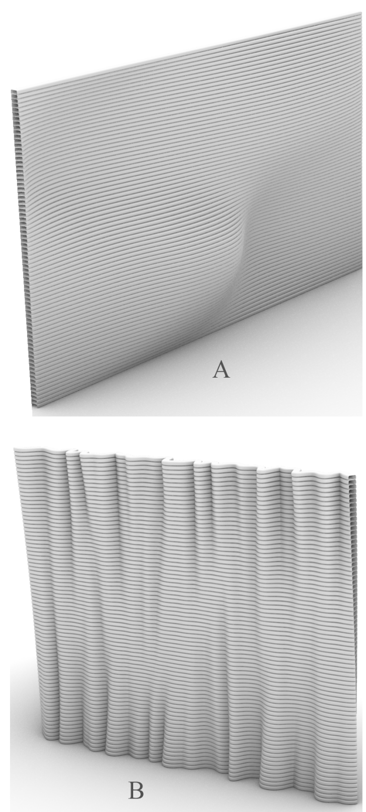

Figure 6 Curved walls A & B for 3D concrete printing

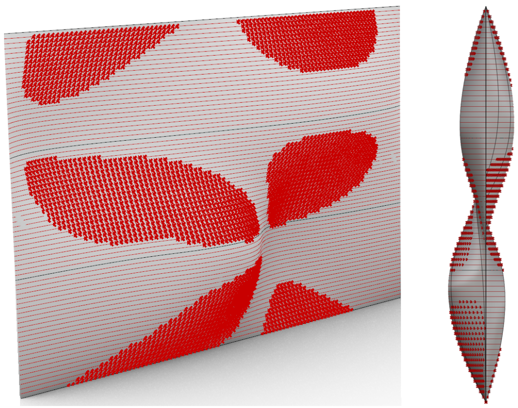

Figure 7 The points exceeded the max lean angle shown in red dots on the perspective (left) and elevation (right)

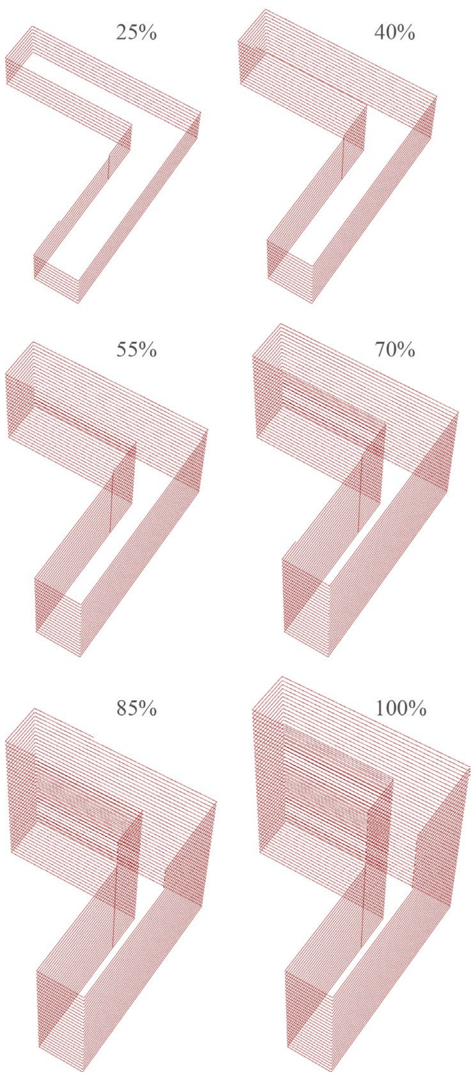

Figure 8 Printing paths animated by dragging a slider in Grasshopper

The path verification module also provides an interface to animate the printing paths so the user can visually verify whether the paths progress as expected. Figure 8 shows six of the frames of an animated printing path as the user drags the slider that controls the printing progress. The printing process from start to end can be easily shown in 1,000 or more total frames which allows the users to investigate the tool path in greater detail.

G-code Generation Module

Once the paths are verified to be correct, the g-code generation module generates two g-code files, one for a 3D concrete printer and the other for an FDM printer to print a scaled model to physically simulate the printing process. The two g-code files are from the same tool paths so the movement of the nozzles of the 3D concrete printer and the FDM printer are expected to be the same but at different scales. The scale is determined by the ratio of the nozzle sizes. For example, if the 3D concrete printer has a cylindrical nozzle with a diameter of 40mm and the FDM printer has a nozzle with a diameter of 0.4mm, the scale is 1:100.

A g-code file is comprised of three parts: header, body, and footer (figure 9). In the g-code file for the 3D concrete printer, the header contains the information related to the positioning system (absolute or relative) and tool selection which is the default nozzle; the body contains the coordinates of the tool path infliction points and the speed of nozzle movement; and the footer contains the nozzle path to the dump point and commands to end printing. If the concrete pump and the 3D printer do not communicate, the pump does not automatically stop at the end of the 3D printing session, so the printer nozzle needs to swiftly move to a dump point while material is being extruded out of the nozzle. In the g-code file for the FDM printer, the header contains the information related to the positioning system, the temperature of the nozzle and bed, and the material priming process; the body of the g-code contains coordinates of the *scaled-down* tool path and the speed of nozzle movement; and the footer contains the commands to end printing and to cool down the nozzle and bed. While the g-code body and footer can be similar, the header can greatly vary depending on the printer and slicer software.

Header

```
G90
M82
T0
; end of header code
```

Body

```
G1 X760 Y760 F3360
; layer 1, Z =20
G1 Z20 F750
G1 X760 Y760 F3360
G1 X1580 Y760
G1 X1580 Y1491
G1 X1399 Y1491
G1 X1399 Y940
G1 X760 Y940
G1 X760 Y760
;layer end
; layer 2, Z =40
G1 Z40 F750
G1 X760 Y760 F3360
G1 X1580 Y760
```

⋮

Footer

```
; begin footer code
G91 ;relative
G1 Z30 ;go up 30mm
;go to dump position
G90 ;absolute
G1 X472 Y413
G92 A0
```

Figure 9 A sample 3DCP g-code file showing header, body, and footer

Test printing the same paths at a smaller scale on an FDM printer is useful for physically simulating the nozzle movement of a 3D concrete printer. Any unexpected nozzle movement can be detected on the FDM printer. The g-code generation module also estimates the total printing time and total material use.

Pilot Study

We conducted a pilot study to verify the effectiveness of the proposed system. The target print is an L-shaped corner of a shed at 860mm (L) x 770mm (W) x 460mm (H) with a 220mm wall thickness. The digital model of the wall is shown in figure 10. The 3D concrete printer we used is an Erectorbot with a nozzle diameter of 40mm. The mixer and pump are manufactured by Ventures Equipment. In this setup, there is no communication between the pump and the 3D printer. The 3D PLA printer we used is a Prusa MK3S+ with a nozzle diameter of 0.4mm. The scale factor is the ratio of the nozzle diameters, i.e., 0.4mm/40mm or a scale factor of 1:100. The slicer module generated two g-code files, one for the Erectorbot and the other for the Prusa printer. The path verification module did not automatically report any potential failing points because the wall is vertical, so the lean angle is 0. Curvilinear walls need to be tested in the future. We did identify one error by visually checking the animation. After correcting the error, we printed the scaled model (8.6mm x 7.7mm x 2.2mm) with the Prusa printer (figure 11). We then sent the full-size G-code to the concrete printer and successfully printed the entire file (figure 12).

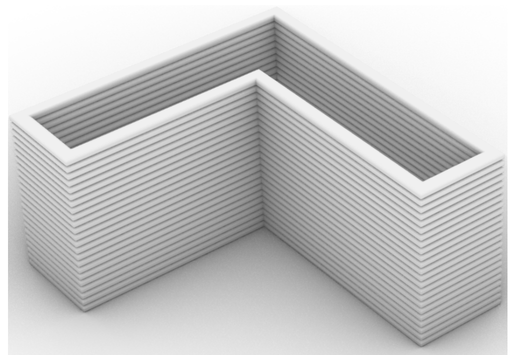

Figure 10 An L-shaped wall for pilot testing. Printing dimensions: 860mm (L) x 770mm (W) x 460mm (H)

3D printing this sample wall in concrete took 4-6 people about three hours (one hour of preparation, 25 minutes of test run without material, 25 minutes of printing, and one hour of cleaning) and more than a dozen 50-lb bags of concrete mix. In comparison, 3D printing the scaled PLA model only took one person four minutes (three minutes for printer warmup and one minute for printing) and 0.3 gram of PLA. The cost of validating the machine movement with a PLA printer is minuscule compared to the actual printing job with concrete.

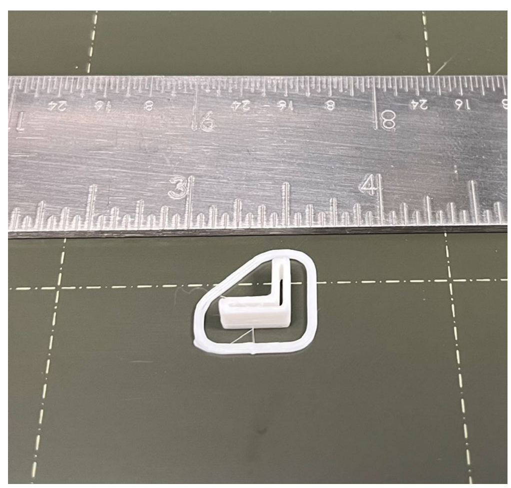

Figure 11 The scaled model (1:100) of the L-shaped wall printed with a Prusa PLA printer. This scaled model was printed with the same toolpaths as the one used for the 3D concrete printer to visually inspect the toolpaths.

Figure 12 The full-size concrete wall printed with the Erectorbot 3D concrete printer

Discussion

Industry generally classifies two kinds of 3DCP materials which are composite and cementitious. As described above in the introduction, 3D printing has a long history and can provide an intentionally scaled material reference point for testing design g-code. The resources and time required are significantly less than what is required in a full-scale cementitious test as described in the previous section. This does not diminish the value or challenges required to successfully perform full-scale cementitious printing, but it does allow for protocols to test the workflow very efficiently to then focus on the combined system involving mixing, pumping, and printing.

Design of the built environment has utilized scale drawings and models as formal instruments of service longer than digital processes and workflows have been available. This familiarity allows for a process bridge while automation and robotic systems advance, and humans-in-the-loop are actively involved in the process, such as preparing custom slicing scripts that respond to particular design or performance criteria. This current process needs protocols for quality, safety, and predictable results.

Using the most common desktop 3D printing nozzle diameter provides an additional familiarity with a 1:100 scale reference being effectively close to a 1/8” = 1’-0” architectural scale. Being able to incorporate designs into a familiar workflow allows for context and material methods beyond 3DCP. Scale models can be constructed in many hybrid manners, including various materials, methods, and 3DCP elements and structures. The inclusion of this new technology into design and building can be methodical and iterative to better advance the use of 3DCP additive strategies in the industry.

This integrated approach is particularly valuable as the industry advances digital workflows that include 4D Planning and Integrated Project Delivery. The capacity to incorporate machine movement, and consumables with multiple activities on site will be an expectation moving forward. Even more so as multiple robotic utilization on project sites advances and becomes normalized. The ability to model, iterate, study, simulate, and understand planned robotic actions and movements on project sites will be critical for site planning, project delivery, and safety protocols.

Conclusion

In this research, we investigated an integrated system to simulate the 3DCP process digitally and physically. A pilot study showed that it was able to screen certain human-made errors and thus improve the success rate of 3DCP jobs and reduce the potential risks to the concrete printer and the operators. More pilot studies are needed to further identify potential issues and improve the reliability of this system. Nonetheless, this study demonstrated a novel approach to identifying potential failures in 3D concrete printing through software screening and physical test printing. The software screening algorithm presented in the study can detect geometric abnormalities that can cause failure due to the limited lean angle using concrete as the printing material. 3D printing a scaled model with thermoplastic can be an efficient way to verify the tool paths before sending the actual printing job to a 3D concrete printer.

The next step is to investigate an automated workflow between the mixer, pump, and printer. Future studies also include additional scale studies with desktop PLA printers using readily accessible nozzles at .6mm (1:63, close to 3/16” = 1’-0”) and .8mm (1:50, close to ¼"=1’-0”) and even larger 1.2mm (1:30, close to 3/8” = 1’-0”) nozzle size to understand the larger scale potentials and utilization for expanding the integrating system. Additional digital prototyping techniques using a larger scale to include full-scale visualizations in extended reality will also be tested for additional integrated system values.

Another area in which current 3D printing technology can positively impact future integrated 3DCP workflow is in multiple material applications. Basing strategies for an integrated 3DCP approach on desktop 3D printers that can print with multi-materials and colors will provide strategies for working with machines that can do more than just the 3DCP operations. Machines are expected to automate additional tasks such as structural elements, insulation materials, finishing, millwork, furnishing, and other details. The complex nature of robotics operations will require a sophisticated and advanced integrated 3DCP system that will incorporate these layered logics in multi-material 3D printing systems and advanced multi-tool CNC operations.

Acknowledgment

This research is funded by the American Recovery & Reinvestment Act of 2009 (ARRA) as a grant from Iowa Economic Development Authority.

References

Autodesk. 2004. Fusion 360 CAM. https://www.autodesk.com/products/fusion-360/

Breseghello, L. and Naboni, R., 2022. Toolpath-based design for 3D concrete printing of carbon-efficient architectural structures. Additive Manufacturing, 56, p.102872.

Bukkapatnam, S., Mander, J., Paal, S., Pei, Z., & Zeng, L. 2017. Workshop Report—NSF Workshop on Additive Manufacturing (3D Printing) for Civil Infrastructure Design and Construction. National Science Foundation (NSF), Alexandria, VA.

Cobod. 2023. Global Market of 3D Printed Buildings. https://cobod.com/global-inventory-3d-printed-buildings/

CyBe Construction. 2004. Chysel on Food4Rhino. https://www.food4rhino.com/en/app/chysel

Hou, S., Duan, Z., Xiao, J., & Ye, J. 2020. A review of 3D printed concrete: Performance requirements, testing measurements and mix design. Construction and Building Materials, 121745.

ISO/ASTM International. 2023. Additive Manufacturing for Construction - Qualification principles - Structural and infrastructure elements [ISO/ASTM 52939:2023(E)]. West Conshohocken, PA. ASTM International. https://www.iso.org/standard/81177.html

Kodama, H., 1981. Automatic method for fabricating a three-dimensional plastic model with photo-hardening polymer. Review of scientific instruments, 52(11), pp.1770-1773.

Lengua, C.A.G., 2017. History of rapid prototyping. Rapid Prototyping in Cardiac Disease: 3D Printing the Heart, pp.3-7.

Luo, W. J., Mao, Z. C., Lu, H. Z., Yang, J., Ma, X. C., & Xu, L. J. 2020. Subversion of conventional construction: Building 3D printing technology. IOP Conference Series: Earth and Environmental Science, 531(1), 012005. https://doi.org/10.1088/1755-1315/531/1/012005

Ma, G., Buswell, R., Leal da Silva, W. R., Wang, L., Xu, J., & Jones, S. Z. 2022. Technology readiness: A global snapshot of 3D concrete printing and the frontiers for development. Cement and Concrete Research, 156, 106774. https://doi.org/10.1016/j.cemconres.2022.106774

Weng, Y., Mohamed, N.A.N., Lee, B.J.S., Gan, N.J.H., Li, M., Jen Tan, M., Li, H. and Qian, S., 2021. Extracting BIM information for lattice toolpath planning in digital concrete printing with developed dynamo script: A case study. Journal of Computing in Civil Engineering, 35(3), p.05021001.

Wu, C., Doyle, S., Senske, N., & Evans, P. 2023. Energy Performance Simulation for 3D Concrete Printed Houses. In the proceedings of ARCC (architectural research centers consortium) 2023 International Conference. Dallas, Texas. April 12-15, 2023.

Ghaderi, E., Evans, P., Doyle, S., Senske, N., & Wu, C. 2024. Hygrothermal Behavior of 3D Concrete Printed Wall Assemblies. Proceedings of SimBuild Conference 2024. Denver, Colorado. May21-23, 2024. IBPSA.

Wu, P., Wang, J., and Wang, X. 2016. A critical review of the use of 3-D printing in the construction industry. Automation in Construction, 68, 21–31. https://doi.org/10.1016/j.autcon.2016.04.005

Xu, W., Huang, S., Han, D., Zhang, Z., Gao, Y., Feng, P. and Zhang, D., 2022. Toward automated construction: The design-to-printing workflow for a robotic in-situ 3D printed house. Case Studies in Construction Materials, 17, p.e01442.